

^3He excitations in dilute mixtures with ^4He

R. N. Bhatt

Bell Laboratories, Murray Hill, New Jersey 07974

(Received 10 November 1977; revised manuscript received 28 April 1978)

The deviation of the ^3He quasiparticle spectrum from the Landau-Pomeranchuk parabolic form, seen in neutron scattering, is shown to be accounted for by including the process of roton emission by ^3He quasiparticles in a self-consistent calculation. The normal-fluid density and second-sound velocity (as functions of temperature and concentration of ^3He), calculated from this spectrum (which exhibits no ^3He roton minimum) with no adjustable parameters, are in agreement with experiment.

I. INTRODUCTION

The ^3He quasiparticle spectrum in dilute ^3He - ^4He mixtures was postulated to have a "roton" dip¹⁻³ as in the case of the ^4He excitation spectrum following experimentally observed deviations^{4,5} from the predictions of the parabolic Landau-Pomeranchuk (LP) $\epsilon_q = q^2/2m^*$ spectrum. (Factors of \hbar and k_B will often be omitted from equations.) A fit to the normal-fluid density⁶ gave the ^3He roton parameters as $\Delta_3 = 6.6$ K, $k_3 = 1.95 \text{ \AA}^{-1}$, $\mu_3 = 0.07m_3$ (m_3 is the mass of the ^3He atom). This contention has been challenged recently.⁷⁻⁹ A microscopic calculation of excitations in mixtures⁸ shows negligible shift in the ^4He spectrum due to hybridization with the ^3He quasiparticle spectrum at small ^3He concentration (less than 5-mole %),¹⁰ in agreement with Raman^{11,12} and neutron^{13,14} measurements, but no dips in the ^3He spectrum in second-order perturbation theory. Kummer *et al.*,⁹ have measured the second-sound velocity in mixtures up to 1-mole % ^3He and conclude that a noticeable discrepancy exists between experiment and the prediction of the LP spectrum, which is increased by the addition of a roton dip to the ^3He spectrum.

Recent neutron measurements¹⁴ indicate deviations from the LP spectrum around $q \sim 1.4 \text{ \AA}^{-1}$ to lower energy values, but are inconclusive regarding the existence of a ^3He roton due to resolution problems beyond 1.7 \AA^{-1} . It is the purpose of this paper to show that there is an alternative explanation of the neutron data, which can be reconciled with the normal-fluid density and second-sound results using *no adjustable parameters* and without involving a deep narrow roton minimum.⁶

The basic idea is the following—as the ^3He quasiparticle momentum increases, it approaches the threshold for emission of a ^4He roton. [At the threshold, obtained by drawing a parabola through the ^4He roton with an effective mass ($m^* + \mu_4$), i.e., the sum of the ^3He quasiparticle and ^4He roton

masses, the quasiparticle emits a roton and continues traveling with it.] The threshold causes a bendover of the ^3He spectrum in the same manner as the threshold for decay of a ^4He excitation into two rotons.¹⁵ However, the phase space for decay is not as large (the imaginary part of the self-energy has a $(\epsilon - \epsilon_{\text{th}})^{1/2}$ behavior), and the bendover is less dramatic.

The vertex for this decay is the same as the vertex for virtual decay of a $q \sim 0$ ^3He quasiparticle into a ^4He roton and ^3He quasiparticle, which dominates the renormalization of the ^3He quasiparticle mass.¹⁶ Thus, the renormalized mass (known from experiment) can be used to determine the vertex, and the ^3He spectrum can be calculated self-consistently, using a zero temperature Green's-function formalism.

The calculation shows a single quasiparticle pole in the ^3He Green's function below a roton quasiparticle continuum for q less than a critical wave vector q_c . As the pole approaches the continuum, it transfers spectral weight to the continuum and ceases to exist as a well-defined excitation beyond q_c . Instead, there is a broad peak in the spectral function $S(q, \omega)$ which may be thought of as a quasiparticle with finite lifetime even at zero temperature and concentration. However, the thermodynamic quantities at low temperature are not sensitive to minor modifications of the spectrum beyond q_c and so it suffices to accurately parametrize the quasiparticle spectrum below q_c (and reasonably beyond) to calculate the normal-fluid density and second-sound velocity to the accuracy of the present experiments.

II. THEORETICAL DETAILS

The Hamiltonian of the system can be written

$$\mathcal{H} = \mathcal{H}_0 + \mathcal{H}_{\text{int}}, \quad (1)$$

where

$$\mathcal{H}_0 = \sum_{\mathbf{k}} \omega_{\mathbf{k}} b_{\mathbf{k}}^\dagger b_{\mathbf{k}} + \sum_{\mathbf{q}} \epsilon_{\mathbf{q}}^0 c_{\mathbf{q}}^\dagger c_{\mathbf{q}} \quad (2a)$$

is the noninteracting part (b^\dagger and c^\dagger create ⁴He excitations and ³He particles, respectively, while ω_k and $\epsilon_q^0 = q^2/2m_3$ are the corresponding energies) and

$$\mathcal{H}_{\text{int}} = \sum_{\vec{k}, \vec{q}} \gamma_k (b_{\vec{k}}^\dagger + b_{-\vec{k}}) c_{\vec{q}}^\dagger c_{\vec{q} + \vec{k}} \quad (2b)$$

is the interaction between ³He particles and ⁴He excitations.

One may obtain Eq. (2b) from a bare interaction between ³He and ⁴He particles; this gives³

$$\gamma_k \sim k^2(1 - S_k^2)/S_k^{3/2}, \quad (3)$$

where S_k is the ⁴He liquid-structure factor.¹⁷ Thus, $\gamma_k \sim \sqrt{k}$ for small k , while it has a peak near the roton wave vector. At large k , $S_k \rightarrow 1$ and γ_k falls off rapidly.

The exact Green's function for the ³He quasiparticle is given by Dyson's equation [see Fig. 1(a)]

$$G(\vec{q}, \omega) = G_0(\vec{q}, \omega) + G_0(\vec{q}, \omega) \Sigma(\vec{q}, \omega) G(\vec{q}, \omega), \quad (4)$$

where

$$\Sigma(q, \omega) = i \int \frac{d^3k}{(2\pi)^3} \frac{d\omega'}{(2\pi)} \gamma_k \Gamma_{\vec{k}\vec{q}} D(\vec{k}, \omega') G(\vec{q} - \vec{k}, \omega - \omega'). \quad (5)$$

Here $\Gamma(\vec{k}, \vec{q})$ is the proper renormalized vertex,¹⁸ γ_k is the bare vertex, and the proper self-energy Σ has renormalized ³He quasiparticle and phonon-roton propagators G and D .¹⁹

$$G_0(\vec{q}, \omega) = \frac{\Theta(q - k_F)}{\omega - \epsilon_q^0 + i\eta} + \frac{\Theta(k_F - q)}{\omega - \epsilon_q^0 - i\eta} \quad (6a)$$

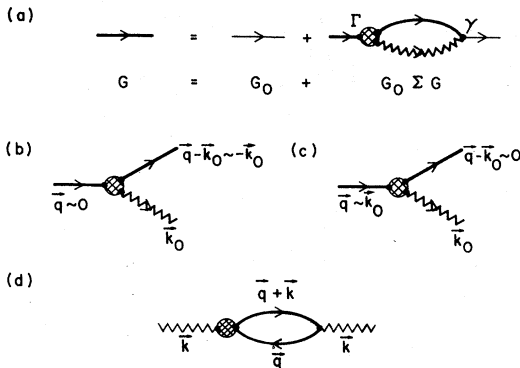


FIG. 1. (a) Dyson's equation; (b) and (c) vertices for $q \sim 0$ and $q \sim k_0$ quasiparticles, respectively; and (d) usual diagram for calculation of hybridization effects. Wavy and straight lines represent ⁴He and ³He propagators. Renormalized (unrenormalized) propagators are in bold (light).

and

$$D_0(\vec{k}, \omega) = \frac{1}{\omega - \omega_k + i\eta} - \frac{1}{\omega + \omega_k - i\eta} \quad (6b)$$

are the unrenormalized (bare) propagators. The factor $\frac{1}{2}\omega_k$ which conventionally appears in D_0 has been incorporated into the definition of the vertices.

For small concentrations of ³He, the renormalization of the ⁴He spectrum is negligible (~ 0.2 K for molar concentration $x \sim 5\%$), so $D(\vec{k}, \omega)$ may be approximated by $D_0(\vec{k}, \omega)$ in the limit $x \rightarrow 0$. For the ³He intermediate state [Eq. (5)] we take the form [Eq. (6a)] with ϵ_q^0 replaced by $\epsilon_q^0 = q^2/2m^*$ for (approximate) self-consistency.²⁰ Within the accuracy of this calculation, it suffices to approximate the ⁴He spectrum by

$$\omega_k = \begin{cases} ck(\text{phonons}), & k < k_1 = 1.3 \text{ \AA}^{-1}, \\ \Delta + (k - k_0)^2/2\mu_4(\text{rotons}), & k_1 < k < k_2 = 2.5 \text{ \AA}^{-1} \end{cases} \quad (7)$$

where k_1 is the point of intersection of the phonon and roton branches, and k_2 the zero of γ_k after the peak in S_k . $c = 238$ m/sec, $\Delta = 8.6$ K, $\mu_4 = 0.16m_4$.

A consideration of the form [Eq. (3)] for γ_k suggests the approximation of one pair of vertices $\gamma_{\text{ph}}(k)$ and $\Gamma_{\text{ph}}(k) \sim \sqrt{k}$ for phonons, and another γ_r and Γ_r (constants) for rotons. If the ratio of the renormalized vertices [$\Gamma_{\text{ph}}(k)/\Gamma_r$] is of the order of the ratio of the unrenormalized ones [$\gamma_{\text{ph}}(k)/\gamma_r$], most of the ³He mass renormalization turns out to be due to rotons in the intermediate state, so the exact magnitude of the phonon vertex is not crucial. We shall work out results for the two cases,

$$\Gamma_{\text{ph}} = 0 \quad (8a)$$

and

$$\Gamma_{\text{ph}}(k)/\Gamma_r = \gamma_{\text{ph}}(k)/\gamma_r = 2.4k^{1/2} (k \text{ in } \text{ \AA}^{-1}). \quad (8b)$$

In the above discussion, it has been possible to suppress the q dependence (distinct from the dependence on k , the momentum transfer) of Γ , because the q dependence of the self-energy is found to be dominated by rotons in the intermediate state. Thus the vertex Γ for small q , which determines most of the mass renormalization [Fig. 1(b)], and $q \sim k_0$ [Fig. 1(c)], which determines the bendover, are the same²¹; in the intermediate q region, the approximation is less accurate but the results should still be reasonable.

With these approximations, the ^3He self-energy in the dilute zero-temperature ($T, \epsilon_F \rightarrow 0$) limit becomes the sum of phonon and roton terms,

$$\Sigma(q, \epsilon) = \Sigma_{\text{ph}}(q, \epsilon) + \Sigma_{\text{roton}}(q, \epsilon), \quad (9)$$

with

$$\Sigma_{\text{roton}}(q, \epsilon) = \frac{\gamma_r \Gamma_r}{4\pi^2} \int_{k_1}^{k_2} k^2 dk \int_{-1}^{+1} \frac{d \cos \theta}{\epsilon - (\tilde{q} - \tilde{k})^2 / 2m^* - \Delta - (k - k_0)^2 / 2\mu_4 + i\eta}, \quad (10b)$$

where θ is the angle between \tilde{q} and \tilde{k} , which may be evaluated exactly. We have used $\gamma_{\text{ph}}(q)\Gamma_{\text{ph}}(k) \sim k$; thus the prefactor $[\gamma_{\text{ph}}(q)\Gamma_{\text{ph}}(q)/4\pi^2 q]$ in Eq. (10a) is a constant. The imaginary part due to phonons $\Sigma_{\text{ph}}^I(q, \epsilon_q)$ vanishes for $q < m^*c$ ($\sim 2.7 \text{ \AA}^{-1}$), while that due to rotons becomes nonzero above a threshold energy:

$$\epsilon_{\text{th}}(q) = \Delta + (q - k_0)^2 / 2(m^* + \mu_4), \quad (11)$$

$$\Sigma_{\text{ph}}(q, \epsilon) = \frac{\gamma_{\text{ph}}(q)\Gamma_{\text{ph}}(q)}{4\pi^2 q} \int_0^{k_1} k^3 dk \times \int_{-1}^{+1} \frac{d \cos \theta}{\epsilon - (\tilde{q} - \tilde{k})^2 / 2m^* - ck + i\eta}, \quad (10a)$$

and

$$\Sigma_{\text{roton}}^I(q, \epsilon) = \begin{cases} 0, & \epsilon \leq \epsilon_{\text{th}} \\ -\frac{\gamma_r \Gamma_r}{4\pi^2} \frac{\sqrt{m^* \mu_4}}{(1 + \mu_4/m^*)^2} \left(\frac{k_0 + \mu_4}{q + m^*} \right) \\ \quad \times \sqrt{2(m^* + \mu_4)(\epsilon - \epsilon_{\text{th}})}, & \epsilon > \epsilon_{\text{th}}. \end{cases} \quad (12)$$

The real part of the self-energy Σ^R is given by

$$\Sigma^R = \Sigma_{\text{ph}}^R + \Sigma_{\text{roton}}^R, \quad (13)$$

with

$$\Sigma_{\text{ph}}^R(q, \epsilon) = \left(\frac{\gamma_{\text{ph}}(q)\Gamma_{\text{ph}}(q)}{4\pi^2 q} \right) \frac{m^*}{q} \left[\frac{1}{3} \left(k_1^3 \ln \left| \frac{m^*c + \frac{1}{2}k_1 - q}{m^*c + \frac{1}{2}k_1 + q} \right| + 8(m^*c - q)^3 \ln \left| \frac{m^*c + \frac{1}{2}k_1 - q}{m^*c - q} \right| + 8(m^*c + q)^3 \ln \left| \frac{m^*c + \frac{1}{2}k_1 + q}{m^*c + q} \right| \right. \right. \\ \left. \left. - 2qk_1^2 + 16m^*cqk_1 + 4m^* \left(\epsilon - \frac{q^2}{2m^*} \right) \left((m^*c - q) \ln \left| \frac{m^*c + \frac{1}{2}k_1 - q}{m^*c - q} \right| \right. \right. \right. \\ \left. \left. \left. - (m^*c + q) \ln \left| \frac{m^*c + \frac{1}{2}k_1 + q}{m^*c + q} \right| \right) \right) + O \left(\left(\frac{\epsilon - q^2}{2m^*} \right)^2 \right) \right], \quad (14a)$$

$$\Sigma_{\text{roton}}^R(q, \epsilon) = \left(\frac{\gamma_r \Gamma_r}{4\pi^2} \right) \frac{m^*}{q} \left[\left(\frac{1}{2}k_2^2 + \mu \Omega \right) \ln \left| \frac{k_2^2 - 2\mu c_1 k_2 + 2\mu \Omega}{k_2^2 - 2\mu c_2 k_2 + 2\mu \Omega} \right| - \left(\frac{1}{2}k_1^2 + \mu \Omega \right) \ln \left| \frac{k_1^2 - 2\mu c_1 k_1 + 2\mu \Omega}{k_1^2 - 2\mu c_2 k_1 + 2\mu \Omega} \right| \right. \\ \left. - \mu^2 c_1^2 \ln \left| \frac{k_2^2 - 2\mu c_1 k_2 + 2\mu \Omega}{k_1^2 - 2\mu c_1 k_1 + 2\mu \Omega} \right| + \mu^2 c_2^2 \ln \left| \frac{k_2^2 - 2\mu c_2 k_2 + 2\mu \Omega}{k_1^2 - 2\mu c_2 k_1 + 2\mu \Omega} \right| + \frac{2\mu q}{m^*} (k_2 - k_1) \right. \\ \left. + 2\mu c_1 (2\mu \Omega - \mu^2 c_1^2)^{1/2} \left(\tan^{-1} \frac{k_2 - \mu c_1}{(2\mu \Omega - \mu^2 c_1^2)^{1/2}} - \tan^{-1} \frac{k_1 - \mu c_1}{(2\mu \Omega - \mu^2 c_1^2)^{1/2}} \right) \right. \\ \left. - 2\mu c_2 (2\mu \Omega - \mu^2 c_2^2)^{1/2} \left(\tan^{-1} \frac{k_2 - \mu c_2}{(2\mu \Omega - \mu^2 c_2^2)^{1/2}} - \tan^{-1} \frac{k_1 - \mu c_2}{(2\mu \Omega - \mu^2 c_2^2)^{1/2}} \right) \right], \quad (14b)$$

where $c_1 = k_0/\mu_4 - q/m^*$, $c_2 = k_0/\mu_4 + q/m^*$, $\mu = \mu_4 m^*/(\mu_4 + m^*)$, and $\Omega = \Delta + k_0^2/2\mu_4 - \epsilon + q^2/2m^*$. In Eq. (14a), the self-energy has been truncated at the lowest-order term in deviations from the parabolic form which is accurate to the same degree as replacement of the intermediate ^3He state by the LP form. Inclusion of the $O((\epsilon - q^2/2m^*)^2)$ term leads to changes which are much smaller than the differences between the results for the two approximations in Eq. (8). The factor inside the square root, in the last term in Eq. (14b), is proportional to $(\epsilon_{\text{th}} - \epsilon)$, and thus Σ_{roton}^R has a $\sqrt{\epsilon_{\text{th}} - \epsilon}$ term, as expected from the result for the

imaginary part [Eq. (12)]. [Also note that ϵ as it appears on the right-hand side of Eqs. (14) is measured from the renormalized zero of energy.]

For wave vectors q less than a certain value q_c [such that the renormalized quasiparticle energy determined self-consistently from Eq. (15) lies below $\epsilon_{\text{th}}(q)$ defined in Eq. (11)], the renormalized Green's function has a pole at an energy given by

$$\epsilon_q = q^2/2m_3 + \Sigma^R(q, \epsilon_q) - \Sigma^R(0, 0), \quad (15)$$

where an uninteresting constant shift has been removed. As expected, as q approaches q_c , the term $\sqrt{\epsilon_{\text{th}}(q) - \epsilon_q}$ in Σ_{roton}^R arising from the emis-

sion of rotons by ³He quasiparticles causes a bendover of the single quasiparticle pole in the Green's function. However, the (finite) bendover term cannot sustain a pole below $\epsilon_{th}(q)$ beyond a critical wave vector q_c , and the single quasiparticle pole merges into the roton-quasiparticle continuum, developing a finite line width even at zero temperature and concentration. Using the $\sqrt{\epsilon_{th} - \epsilon}$ nature of the bendover term in Σ^R , the quasiparticle pole may be shown to approach $\epsilon_{th}(q)$ tangentially, with a spectral weight $Z_q \sim (1 + d\Sigma/d\epsilon)_{\epsilon=\epsilon_q}^{-1}$ decreasing linearly to zero as $q \rightarrow q_c$.

The above results indicate that shifts in the ⁴He spectrum near the roton minimum at larger x , due to hybridization with the ³He quasiparticle branch [Fig. 1(d)], cannot simply be calculated by using $q^2/2m^*$ or even ϵ_q in the intermediate ³He state, but must properly take into account finite lifetime effects of the ³He intermediate state. Thus, the shift of spectral weight to higher energies would tend to cancel level repulsion from the quasiparticle pole.

Before going on to comparison with experiment, we note that for finite concentrations x , the second term on the right-hand side of Eq. (6a) should be used instead of the first for quasiparticles with $q < k_F$. This leads to, in addition to a small fractional increase of the Fermi velocity of order $k_F^3 \propto x^2$, a rather weak singularity at the Fermi surface (for $T = 0$) of the form $(1 - q/k_F)^3 \ln |1 - q/k_F|$ of the same order of magnitude. However, this would be washed away at finite temperature and probably not be noticeable at least for the weaker solutions.

III. RESULTS AND COMPARISON WITH EXPERIMENT

For a given ratio of phonon and roton coupling constants [Eqs. (8a) and (8b)], the renormalized spectrum depends on only one parameter—the product $\gamma_r \Gamma_r$. Determining that from the experimental renormalization of the ³He mass ($m_3 \rightarrow 2.3m_3$) separately in each case [Eqs. (8a) and (8b)], the ³He quasiparticle spectrum is obtained by solving the transcendental equation [Eq. (15)] on a computer. The results are shown in Fig. 2 for the two cases $\Gamma_{ph} = 0$ and $\Gamma_{ph}/\gamma_{ph} = \Gamma_r/\gamma_r$, along with the neutron results. The magnitude of the bendover calculated is seen to be well within the experimental results, while the pure parabolic spectrum is not. Comparison is limited by the resolution of the neutron data and by the width $4\sqrt{\epsilon_F \epsilon_q}$ of the quasiparticle hole continuum which would be present at finite ³He concentration, even in an ideal neutron experiment.

In order to evaluate the normal-fluid density and second-sound velocity in the dilute mixtures,

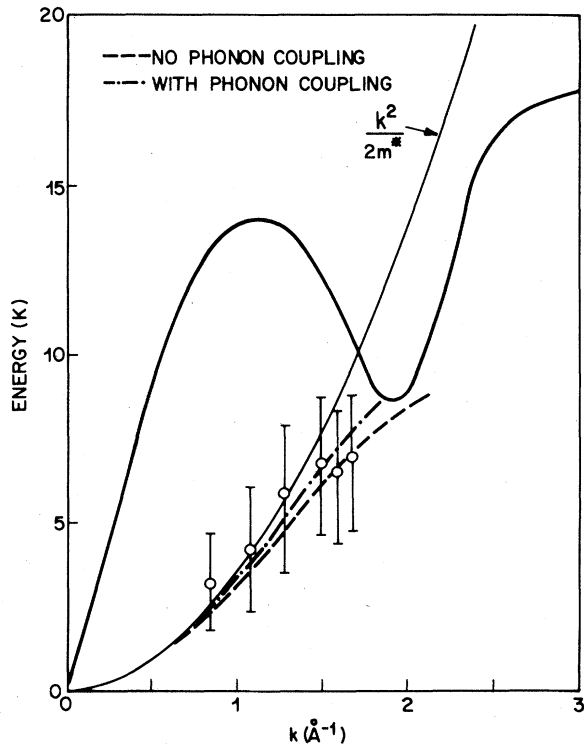


FIG. 2. Dashed and dot-dashed curves are the ³He quasiparticle spectrum calculated using approximation discussed in text. Also shown are the LP parabolic curve and the spectrum of pure ⁴He. The open circles are neutron results on $x = 6$ -mole % solution.

we parametrize the ³He quasiparticle spectrum by

$$\epsilon_q = \begin{cases} (q^2/2m^*)(1 - q^2/Q^2), & q < q_c \\ (q^2/2m^*)(1 - q_c^2/Q^2), & q > q_c \end{cases}, \quad (16)$$

where q_c is the point where the spectrum intersects $\epsilon_{th}(q)$, and Q determines the deviation of the spectrum from the parabolic form below q_c . The expression [Eq. (16)] (for $q < q_c$) constitutes the first two terms in an expansion of ϵ_q in powers of q^2 and is found to be a surprisingly accurate approximation of the deviation of calculated spectrum over the relevant range of momenta ($0.5 \text{ \AA}^{-1} < q < 1.7 \text{ \AA}^{-1}$).²² The form for $q > q_c$ (chosen to coincide at q_c) is also a reasonable approximation to the damped mode above q_c , and results are not sensitive to minor variations of the form selected. Besides, the one-parameter (Q) form appears to be entirely adequate within the accuracy of the present theory (cf. the differences in the spectrum calculated for the two cases in Fig. 2), and the scatter and accuracy of the present experimental data. Fitting the two cases in Fig. 2 gives $Q = 3.2$ and 3.8 \AA^{-1} .

The normal-fluid density and specific heat due to the ³He quasiparticles are given in terms of the

usual phase space integrals²³

$$\rho_{n3} = \frac{1}{3} \int q^2 \left(-\frac{\partial n}{\partial \epsilon} \right) d\tau_q \quad (17)$$

and

$$C_v \equiv T \left(\frac{dS}{dT} \right)_N = \left(\frac{dE}{dT} \right)_N, \quad (18)$$

where

$$E = \int \epsilon n d\tau_q \quad (19a)$$

and

$$N = \int n d\tau_q. \quad (19b)$$

Here $n = [\exp(\epsilon - \mu)/T + 1]^{-1}$ is the Fermi distribution and $\epsilon(q)$ is the excitation spectrum. For the Landau-Pomeranchuk form $\epsilon(q) = q^2/2m^*$, the results are

$$\rho_{n3} = m^* n_3 \quad (20a)$$

and

$$C_v = \frac{3}{2} n_3 k_B, \quad (T \gg \epsilon_F), \quad (20b)$$

where n_3 is the number of ^3He atoms per unit volume and ϵ_F is the Fermi energy.

For a spectrum with a ^3He roton dip

$$\epsilon(q) = \Delta_3 + (q - k_3)^2/2\mu_3, \quad (21)$$

in addition to the parabolic form, one obtains [to $O(e^{-\Delta_3/T})$]

$$\rho_{n3} \simeq m^* n_3 \left[1 + \alpha \left(\frac{k_3^2}{2m^*T} - \frac{3}{2} \right) \right], \quad \epsilon_F \lesssim T \ll \Delta_3, \quad (22a)$$

$$C_{v3} \simeq \frac{3}{2} n_3 k_B \left[1 + \alpha \left(\frac{\Delta_3^2}{T^2} - \frac{2\Delta_3}{T} \right) \right], \quad \epsilon_F \ll T \ll \Delta_3, \quad (22b)$$

where

$$\alpha = (2\hbar^2 k_3^2 / 3m^* k_B T) \sqrt{\mu_3/m^*} e^{-\Delta_3/T}. \quad (23)$$

In obtaining the above equations, the ^3He quasi-particle number has been conserved, and therefore the "roton" contributions to Eqs. (22) are not the same as for ^4He . In addition, while the expression for specific heat [Eq. (22b)] is true only for $T \gg \epsilon_F$, the result for normal-fluid density [Eq. (22a)] is very good even at low temperatures because Eq. (20a) is exact for the LP spectrum for all temperatures, and so errors in Eq. (22a) are $O(e^{-\Delta_3/\epsilon_F})$.

For the spectrum [Eq. (16)], one may work out expressions by expanding the spectrum about a parabolic form in order to evaluate thermal in-

tegrals. This amounts to a power series expansion in T/T_0 , where $T_0 = Q^2/2m^*$; however, because of the spectrum given by the first part of Eq. (16) bends over at large q , one cannot let q_c go to infinity and the analytical result is not particularly advantageous with finite q_c . Therefore, the normal-fluid density and specific heat have been evaluated numerically using Eqs. (17)–(19), for the spectrum given by Eq. (16).

The second-sound velocity for dilute mixtures is given by²³:

$$u_{II}^2 = \frac{\rho_s T}{\rho_n} \left[\frac{(\sigma_4 + k_B x/m_4)^2}{C} + \frac{k_B x}{m_4} \right], \quad (24)$$

where ρ_n and ρ_s are the total normal-fluid and superfluid densities, σ_4 is the ^4He entropy, and C is the total specific heat per unit mass of the solution, and x is the molar concentration of ^3He .

Turning now to the normal-fluid density, we fit the data⁴ for $x = 11\%$ using the normal-fluid density for ^4He from Bendt *et al.*²⁴ for all three spectra [Eq. (16), LP, and LP plus Eq. (21)]. In each case, m^* is determined from the data at the lower temperatures. The data are seen to be fit as well (Fig. 3) by the spectrum (16) with $Q = 3.4 \text{ \AA}^{-1}$ and $m^* = 2.1m_3$ as the three-parameter roton fit ($\Delta_3 = 6.6 \text{ K}$, $k_3 = 1.95 \text{ \AA}^{-1}$, $\mu_3 = 0.07m_3$) with $m^* = 2.25m_3$. The Landau-Pomeranchuk spectrum, however, underestimates the normal-fluid density at the highest temperatures by about 20% of the zero-temperature ρ_{n3} .

In Fig. 4(a), we compare the second-sound velocity determined experimentally⁹ for the $x = 0.71\%$ solution with the predictions [from Eq. (24)] of the three spectra—parabolic ($m^* = 2.4m_3$), parabolic plus roton ($m^* = 2.4m_3$, roton parameters as above), and Eq. (16) with $Q = 3.4 \text{ \AA}^{-1}$ and $m^* = 2.25m_3$ using pure ^4He data again from Ref. 24. The renormalized masses are again determined by fitting the data at the lowest temperatures and for each spectrum are somewhat higher (by 0.15 m_3) than the previous case. This is not surprising because m^* in general depends on the concentration [through the concentration dependence of $\Sigma^R(q, \epsilon)$ which we have neglected in the present calculation, and also through $^3\text{He} - ^3\text{He}$ interaction omitted in the present model] and a decrease of m^* with increasing concentration has been found experimentally, too.^{6,26} (In addition, any inaccuracy in the determination of x gets lumped into a renormalization of m^* for ρ_{n3} .) As can be seen, Eq. (16) yields a better fit than the parabolic plus roton spectrum, which in turn is in better agreement with experiment than the pure parabolic spectrum.²⁷ Figure 4(b) shows the fits using Eq. (16) with the same parameters as Fig. 4(a), for different concentrations. The small deviations

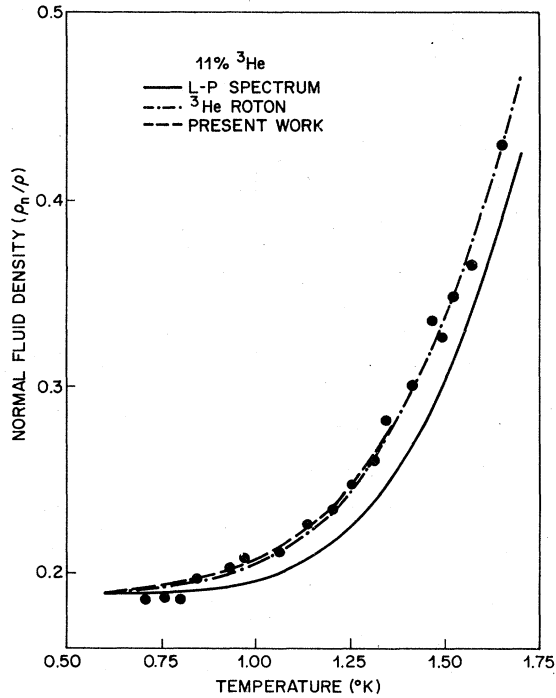


FIG. 3. Total normal-fluid density for $x=11$ -mole % (data of Ref. 4) along with calculations for various forms of the ^3He quasiparticle spectrum. Where the calculation for Eq. (16) is not shown, it agrees with the roton spectrum result to within the width of the lines.

above 1 K are not experimentally significant and do not scale with x (as would be expected for errors in the ^3He spectrum or shift of the ^4He spectrum due to ^3He). We also note that previous second-sound velocity measurements below 0.6 K have been fitted there²⁶ using Eq. (16) with $Q=4.0 \pm 0.8 \text{ \AA}^{-1}$.

IV. CONCLUSIONS

The present work has shown that the deviation of the ^3He spectrum in dilute $^3\text{He} - ^4\text{He}$ mixtures from the Landau-Pomeranchuk parabolic form, seen in neutron scattering, is in agreement with a theoretical estimate of the bendover due to the decay channel $^3\text{He} \rightarrow ^3\text{He} + \text{rotons}$ using a rather simple picture of interaction between ^3He and ^4He . Further, by parametrizing the theoretically calculated spectrum in terms of a single bendover parameter Q , which seems to be adequate to within the accuracy of both experiment and theory at present, the calculated normal-fluid density and second-sound velocity (as functions of temperature and concentration of ^3He) are found to be in agreement with experiment, with essentially no adjustable parameters.

No *a priori* claim can, of course, be made about

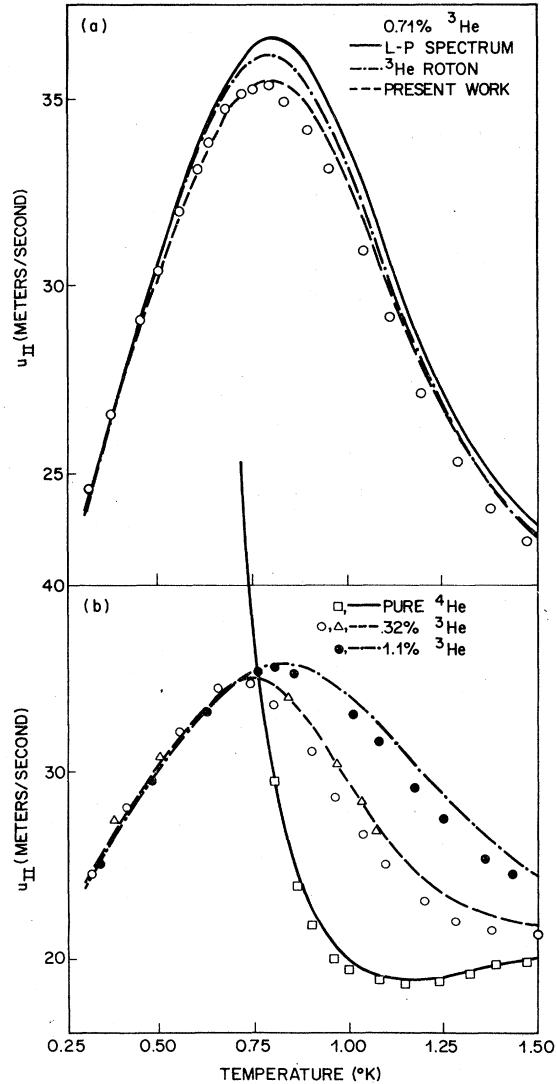


FIG. 4. Second-sound velocity obtained from Eq. (24) (a) in $x=0.71$ -mole % solution using different forms of the quasiparticle spectrum; (b) for different concentrations using the spectrum (9). Data are from Ref. 9 (except triangles from Ref. 25).

quantitative accuracy of the theoretical calculation in view of the original simplifying assumptions about the vertices. However, the essential physics and qualitative nature of the bendover are, we believe, correct and, in view of the remarkable agreement with experiment, a quantitative first approximation. Further refinement of this model at this stage, though, would be little more than a parameter game because of lack of any experimental evidence requiring that and because of the somewhat intractable nature of calculations in a strongly coupled system like the $^3\text{He} - ^4\text{He}$ mix-

tures. On the other hand, both the absence of any pronounced ^3He roton minimum in the calculation, and the amenability of present experimental data to explanation in terms of a spectrum without the minimum, provide incentive for further, more accurate, experimental work on, say, normal-fluid density and specific heat, to determine the quantitative details of the deviation of the ^3He quasiparticle spectrum in mixtures from the parabolic form.

Note added in proof. Recently, after this work was submitted for publication, Greywall has done high-precision specific-heat measurements²⁸ on dilute ^3He - ^4He mixtures ($x = 0.004$ – 1.0 mole %). His results confirm that there are substantial deviations from the results of the LP parabolic spectrum (which increase with temperature, extrapolating to about 15% at 1 K). The data can be fit in

terms of a roton only with unreasonable, concentration-dependent parameters ($\Delta_3 \sim 2.5$ – 3.5 K, $\mu_3 \sim 10^{-3}$ – $10^{-4}m_3$). The deviations are in approximate quantitative agreement with the results based on the spectrum (16) with the present parameters, above 0.3 K. The data do, however, show a small kneelike feature (magnitude $\sim 1\%$) in the specific heat versus temperature plot around 0.2 K, which is not present in the specific heat computed from the parametrized form in Eq. (16).

ACKNOWLEDGMENTS

This work was started while the author was at the Aspen Center for Physics. Helpful discussions with C. M. Varma, R. C. Dynes, V. Narayanamurti, and P. C. Hohenberg are gratefully acknowledged.

- ¹L. P. Pitaevskii, Comments at the U. S.-Soviet Symposium on Condensed Matter, Berkeley, 1973 (unpublished).
- ²C. M. Varma, Phys. Lett. A **45**, 301 (1973).
- ³M. J. Stephen and L. Mittag, Phys. Rev. Lett. **31**, 923 (1973).
- ⁴V. I. Sobolev and B. N. Esel'son, Zh. Eksp. Teor. Fiz. **60**, 240 (1971) [Sov. Phys. JETP **33**, 132 (1971)].
- ⁵B. N. Esel'son, Yu. Z. Kovdrya, and V. B. Shikin, Zh. Eksp. Teor. Fiz. **59**, 64 (1970) [Sov. Phys. JETP **32**, 37 (1971)].
- ⁶V. I. Sobolev and B. N. Esel'son, Zh. Eksp. Teor. Fiz. Pis'ma Red. **18**, 689 (1973) [JETP Lett. **18**, 403 (1973)].
- ⁷J. Slinkman and J. Ruvalds (unpublished) and J. Ruvalds, in *Quantum Liquids* (North-Holland, Amsterdam, 1978), pp. 263–291 have shown that a ^3He roton at 5 K is in disagreement with the data of Ref. 4, and (we believe mistakenly) have come to the conclusion that a roton spectrum is not commensurate with the data of Ref. 4.
- ⁸J. Ruvalds, J. Slinkman, A. K. Rajagopal, and A. Bagchi, Phys. Rev. B **16**, 2047 (1977).
- ⁹R. B. Kummer, V. Narayanamurti, and R. C. Dynes, Phys. Rev. B **16**, 1046 (1977).
- ¹⁰The earlier quantum-hydrodynamic calculation of D. L. Bartley, J. E. Robinson, and V. K. Wong, J. Low Temp. Phys. **12**, 71 (1973) had shown significant modification of the ^4He spectrum due to hybridization with the ^3He quasiparticle branch.
- ¹¹C. M. Surko and R. E. Slusher, Phys. Rev. Lett. **30**, 1111 (1973).
- ¹²R. L. Woerner, D. A. Rockwell, and T. J. Greytak, Phys. Rev. Lett. **30**, 1114 (1973).
- ¹³J. M. Rowe, D. L. Price, and G. E. Ostrowski, Phys. Rev. Lett. **31**, 510 (1973).
- ¹⁴P. A. Hilton, R. Scherm, and W. G. Stirling, J. Low Temp. Phys. **27**, 851 (1977).
- ¹⁵L. P. Pitaevskii, Zh. Eksp. Teor. Fiz. **36**, 1168 (1959) [Sov. Phys. JETP **9**, 830 (1959)].
- ¹⁶This result actually follows from the calculation,

- assuming that the ratio of the renormalized vertices for the phonon and roton is not much greater than that for the unrenormalized ones.
- ¹⁷This depends on identifying the ^4He excitations as density fluctuations, in the spirit of Feynman [Phys. Rev. **94**, 262 (1954)] and Bogoliubov-Zubarev [Zh. Eksp. Teor. Fiz. **23**, 129 (1955) [Sov. Phys. JETP **1**, 83 (1955)]], so higher-order interactions are left out.
- ¹⁸Vertex corrections are not of order of the Fermi momentum k_F , as stated in Ref. 8, and cannot be assumed to be negligible. Thus Eq. (3) should be used only for qualitative trends as regards $\Gamma(\vec{k}, \vec{q})$.
- ¹⁹A. L. Fetter and J. D. Walecka, *Quantum Theory of Many-Particle Systems* (McGraw-Hill, New York, 1971), pp. 402–405.
- ²⁰Actually, a constant should be added to $q^2/2m^*$, due to an overall shift of the spectrum, but since only energy differences enter the calculation of $\Sigma(q, \epsilon_q)$, the constant drops out and may be suppressed to begin with.
- ²¹This assumes that the q dependence of the vertex at small q is dominated by that of the self-energy. There is no *a priori* justification of this, except that using bare vertices gives 80% of the mass renormalization at small q (Ref. 8), and the approximation $\Gamma(\vec{k}, \vec{q}) = \Gamma(k) \neq \gamma_k$ should do better. Besides the agreement with experiment could be viewed as a *posteriori* justification.
- ²²It does slightly overestimate the deviation at small q and underestimate that at larger q . This would imply somewhat lesser deviation from the LP form at lower temperatures and larger at higher temperatures for the calculated spectrum than that given by Eq. (16).
- ²³I. M. Khalatnikov, *Introduction to the Theory of Superfluidity* (Benjamin, New York, 1965), pp. 161–164.
- ²⁴P. J. Bendt, R. D. Cowan, and J. L. Yarnell, Phys. Rev. **113**, 1386 (1959).
- ²⁵J. C. King and H. A. Fairbanks, Phys. Rev. **93**, 21

(1954).

²⁶N. R. Brubaker, D. O. Edwards, R. E. Sarwinski, P. Seligmann, and R. A. Sherlock, *Phys. Rev. Lett.* **25**, 715 (1970).

²⁷This is contrary to the statement of Ref. 9. We believe this is so because the formula for second-sound

velocity used in Ref. 9, as generalized there from the result for Bose excitations, does not correctly keep track of ^3He quasiparticle number conservation (chemical potential) and does not agree with Eq. (24).

²⁸D. S. Greywall, *Phys. Rev. Lett.* **41**, 177 (1978).